Immune complex solubility and size govern Fc-gamma receptor responses: A scalable cell-based reporter system

Haizhang Chen[1,2], Andrea Maul-Pavicic[3,4], Martin Holzer[5], Ulrich Salzer[3], Nina Chevalier[3], Reinhard E. Voll[3,4], Hartmut Hengel[1,2,*] & Philipp Kolb[1,2,*]

[1]Institute of Virology, University Medical Center, Albert-Ludwigs-University Freiburg, Hermann-Herder-Str. 11, 79104 Freiburg, Germany

[2]Faculty of Medicine, Albert-Ludwigs-University Freiburg, 79104 Freiburg, Germany

[3]Department of Rheumatology and Clinical Immunology, Medical Center - University of Freiburg, Faculty of Medicine, University of Freiburg, Hugstetterstr. 55, 79106 Freiburg, Germany

[4]Center for Chronic Immunodeficiency (CCI), Medical Center-University of Freiburg, Faculty of Medicine, University of Freiburg, Breisacherstr. 115, 79106 Freiburg, Germany

[5]Institute for Pharmaceutical Sciences, Albert-Ludwigs-University Freiburg, Hermann-Herder-Str. 9, 79104 Freiburg, Germany

*corresponding authors (Hartmut.hengel@uniklinik-freiburg.de)

One Sentence Summary: This study reveals selective activation of individual Fc-gamma receptors by soluble but not immobilized immune complexes, establishing a novel biomarker for autoimmune disease in humans and mouse models.

Abstract: Fc-gamma receptor (FcγR) activation by soluble IgG immune complexes (sICs) is thought to be a major mechanism of inflammation in certain autoimmune diseases such as systemic lupus erythematosus (SLE). A robust and scalable test system allowing for the detection and quantification of sIC bioactivity is missing. Therefore, we developed a comprehensive reporter cell panel capable of measuring the sIC-mediated activation of individual human and mouse FcγRs. We show that compared to human FcγRs IIB and III, human FcγRs I and IIA lack sensitivity to sICs. Further, the assay proved to be sensitive to sIC stoichiometry and size enabling us to demonstrate for the first time a complete translation of the Heidelberger-Kendall precipitation curve to FcγR responsiveness. This was validated using primary immune cells. The approach was applied to quantify sIC-mediated FcγR activation using sera from SLE patients or from mouse models of lupus and arthritis. Thus, in clinical practice, it can be employed as a toolbox enabling the evaluation of FcγR activation by sICs as a biomarker for disease activity in immune-complex mediated diseases.

Introduction

Immunoglobulin G (IgG) is the dominant immunoglobulin isotype in chronic infections and in antibody-mediated autoimmune diseases. The multi-faced effects of the IgG molecule rely both on the F(ab) regions, which recognize a specific antigen to form immune complexes (ICs), and the constant Fc region (Fcγ), which is detected by Fcγ receptors (FcγRs) found on most cells of the immune system (*1*). When IgG binds to its antigen ICs are formed, which, depending on the respective antigen, are either cell-bound or soluble (sICs). The composition of sICs is dependent on the number of epitopes recognized by IgG on a single antigen molecule and the ability of the antigen to form multimers. Fcγ-FcγR binding is necessary but not sufficient to activate FcγRs since physical receptor cross-linking generally underlies receptor activation (*2-5*). Firmly fixed cell bound ICs are readily able to cross-link FcγRs (*4, 6*). This condition induces various signaling pathways (*7-9*) which in turn regulate immune

cell effector functions (*10, 11*). It is also suggested that sICs can dynamically tune FcγR triggering, implying that changes in sIC size directly impact FcγR responses (*6*). However, the molecular requirements are largely unknown. Also, a functional reproduction of the paradigmatic Heidelberger-Kendall precipitation curve, describing that the molecular size of sICs determined by the antibody:antigen ratio dynamically tunes FcγR activation on and off (*12, 13*), is so far missing.

In contrast to FcγR binding of monomeric ligands without consequences, IC-mediated FcγR cross-linking initiates the full signal cascade followed by immune cell activation or inhibition, resp. (*5, 8, 14, 15*). Human FcγRs are membrane resident receptors recognizing Fcγ. Among all type I FcγRs, FcγRIIB (CD32B) is the only inhibitory one signaling via immunoreceptor tyrosine-based inhibitory motifs (ITIMs) while the activating receptors are associated with immunoreceptor tyrosine-based activation motifs (ITAMs). Another exception is FcγRIIIB (CD16B), which is glycosylphosphatidylinositol (GPI)-anchored (*16-19*). FcγRI (CD64) is the only receptor with high affinity binding to monomeric IgG not associated with antigen and is primarily tasked with phagocytosis linked to antigen processing and pathogen clearance (*20, 21*). All the other FcγRs only efficiently bind to complexed, meaning antigen-bound IgG (*1, 16, 17*). While FcγRI, FcγRIIB and FcγRIIIA are able to recognize sICs, this has not been reported for FcγRIIA (CD32A), rather this receptor has recently been shown to depend on the neonatal Fc receptor (FcRn) or FcγRIIIB (CD16B) to do so (*22, 23*). Activation of FcγRs leads to a variety of cellular effector functions such as antibody-dependent cellular cytotoxicity (ADCC) by natural killer (NK) cells via FcγRIIIA, antibody-dependent cellular phagocytosis (ADCP) by macrophages via FcγRI, cytokine and chemokine secretion by NK cells and macrophages via FcγRIIIA. Further effector responses are reactive oxygen species (ROS) production of neutrophils and neutrophil extracellular traps formation (NETosis) via FcγRIIIB, dendritic cell (DC) maturation and antigen presentation via FcγRIIA and B cell selection and differentiation via FcγRIIB (*10, 24-30*). Consequently, FcγRs connect and

regulate both innate and adaptive branches of the immune system. Various factors have been indicated to influence the IC-dependent FcγR activation profiles, including Fcγ-FcγR binding affinity and avidity (*31*), IgG subclass, glycosylation patterns and genetic polymorphism (*4, 24, 25, 32*), stoichiometry of antigen-antibody-ratio (*6, 30, 33*) and FcγR clustering patterns (*34*). Specifically, Asn297-linked glycosylation patterns of the IgG Fc domain initiate either pro- or anti-inflammatory effector pathways by tuning the binding affinity to activating versus inhibitory FcγRs, respectively (*35*). However, despite being explored in proof-of-concept studies, the functional consequences of these ligand features on a specific receptor are still not fully understood. Therefore, an assay platform allowing for the systematic functional assessment of IC-mediated FcγR activation is strongly required. While a previously developed cell-based assay addresses sIC-mediated activation of the inhibitory FcγRIIB (*36*), a platform allowing for the comprehensive analysis of all FcγRs is missing.

sICs and immobilized ICs represent different stimuli for the immune system (*22, 29*). Soluble circulating ICs are commonly associated with certain chronic viral or bacterial infections (*37, 38*) and autoimmune diseases, such as systemic lupus erythematosus (SLE) or rheumatoid arthritis (RA) (*39-41*). When accumulating and deposited in tissues sICs can cause local damage due to inflammatory responses, classified as type III hypersensitivity (*42*). Typically, sICs related disorders are characterized by systemic cytokine secretion which can be followed by immune cell exhaustion and senescence (*43, 44*). In order to study sIC-dependent activation of FcγRs in detail, we employed a cell-based assay which has been previously utilized to study immobilized ICs (*45*) and adapted it into a sIC sensitive reporter system capable of distinguishing the activation of individual FcγRs and their responses to varying complex size. This approach allowed for the first time a complete reproduction of the Heidelberger-Kendall precipitation curve measuring actual FcγR triggering. The assay enables a quantification of clinically relevant sICs in sera from SLE patients and autoimmune-

prone mice with immune-complex-mediated arthritis and lupus using reporter cells expressing chimeric mouse FcγRs.

Results

Experimental assay setup

The assay used in this study was adapted from a previously described cell-based FcγR activation assay designed to measure receptor activation in response to opsonized virus infected cells (*45*) or therapeutic Fc-fusion proteins (*46*). We complemented the assay setup to enable measurement of sICs when incubated with reporter cells stably expressing the ectodomains of the human FcγR fused to the signaling module of the mouse CD3-ζ chain (FcγRI: Acc# X14356; FcγRIIA(R): Acc# X62572; FcγRIIB/C: Acc# X52473; FcγRIIIA(V): Acc# LT737365). Ectodomains of FcγRIIB and FcγRIIC are identical. Second generation reporter cells were generated to improve stable expression of chimeric FcγRs compared to the transfectants used in the original assay (*45*). To this end, BW5147 cells were transduced as described previously via lentiviral transduction (*45, 47*). Human FcγR expression on transduced cells after puromycin selection is shown in Fig. 1A. FcγR triggering is translated into activation of the reporter cells and measured by quantification of endogenous IL-2 (mIL-2) secretion into the cell culture supernatant using an anti-IL-2 sandwich ELISA as described previously (*45*). In order to employ the original assay, designed to detect ICs on adherent virus-infected cells, for the detection of soluble ICs we first determined the suspension of IgG achieved by pre-incubating a 96 well ELISA microtiter plate with PBS/FCS blocking buffer. To this end, we compared graded concentrations of FCS in the blocking reagent and measured the threshold at which IgG (rituximab, Rtx) was no longer adsorbed to the plate and stayed abundantly in solution. Fig. 1B demonstrates that FCS supplementation to 1% (v/v) or higher is sufficient to keep IgG antibodies in solution and prevents binding to the plastic surface. Using this adapted protocol, the assay now allowed for the sensitive detection and

characterization of FcγR interaction with immobilized ICs versus sICs as shown schematically in Fig. 1C. First, we set out to test if monomeric IgG upon immobilization becomes an operational surrogate for IgG-opsonized cells or immobilized ICs with regard to FcγR activation as suggested before (*48*). As depicted in Fig. 2, there was no qualitative difference in FcγR activation between immobilized Rtx, immobilized ICs (Rtx + rec. CD20) or Rtx-opsonized 293T-CD20 cells, showing that FcγR cross-linking by clustered IgG alone is sufficient for receptor cross-linking and activation. In contrast, sICs formed by monomeric CD20 peptide (aa 141-188) and Rtx failed to activate FcγRs even at very high ligand concentrations. Based on this finding we hypothesized that, in order to generate sICs able to activate FcγRs, antigens have to be multivalent to achieve cross-linking of FcγRs. Of note, to reliably and accurately differentiate between soluble and immobilized triggers using this assay, reagents for the generation of ICs need to be of very high purity and consistent stability. Indeed, only combinations of pharmaceutical therapy grade, i.e. ultra-pure mAbs and pure antigens (purified via size exclusion chromatography) showed reproducible, dose-dependent and specific activation in the reporter assay (data not shown).

Quantification of human FcγR responsiveness to multimeric sICs

To date, there are only few commercially available human IgG-antigen pairs that meet both the above mentioned high grade purity requirements while also providing a multimeric antigen. In order to meet these stipulations of ultra-pure synthetic soluble immune complexes we focused on three pairs of multivalent antigens and their respective mAbs that were available in required amounts enabling large-scale titration experiments; trimeric rhTNFα:IgG1 infliximab (TNFα:Ifx), dimeric rhVEGFA: IgG1 bevacizumab (VEGFA/Bvz) and dimeric rhIL-5: IgG1 mepolizumab (IL-5/Mpz). As lymphocytes express TNFα-receptors I and II while not expressing receptors for IL-5 or VEGFA, we tested whether the mouse lymphocyte derived BW5147 thymoma reporter cell line is sensitive to high concentrations of

rhTNFα. Toxicity testing revealed that even high concentrations up to 76.75 nM rhTNFα did not affect viability of reporter cells (Fig. S1). Next, we measured the dose-dependent activation of human FcγRs comparing immobilized IgG to soluble ICs using the FcγR reporter cell panel (Fig. 3). Soluble antigen or mAb alone served as negative controls showing no background activation even at high concentrations. Immobilized rituximab served as a positive control for inter-experimental reference. We observed that all FcγRs are strongly activated in a dose-dependent manner when incubated with immobilized IgG. Incubating the FcγR reporter cells with sICs at identical molarities showed FcγRIIB/C and FcγRIIIA to be efficiently activated by sICs, while in contrast, FcγRIIA and FcγRI did not respond to sICs. We furthermore observed FcγRIIIA to be efficiently activated by sICs with responses even surpassing those achieved with immobilized IgG for TNFα/Ifx and IL-5/Mpz ICs. FcγRIIB/C showed a generally weaker reactivity towards sICs compared to immobilized ICs, especially at high concentrations whereas an inversion of this order was seen for TNFα/Ifx and VEGFA/Bvz ICs at lower concentrations. IL-5/Mpz, FcγRIIB/C and FcγRIIIA showed similar responsiveness towards immobilized or sICs with a generally stronger activation on immobilized ICs. These findings demonstrate that sICs of different composition vary in the resulting FcγR activation pattern, most likely due to the antigens being either dimeric, trimeric or different in size. As we observed differences in responses to sICs vs. immobilized ICs for individual FcγR-ζ reporter cells, this indicates that FcγR ectodomains alone are already able to differentiate between these triggers. To validate this observation in principle, we determined FcγRIIIA activation using primary human NK cells isolated from PBMCs of healthy donors. NK cells were chosen as they mostly express only one type of FcγR similar to our reporter system. Measuring a panel of activation markers and cytokine responses by flow cytometry, we observed a differential activation pattern depending on ICs being soluble or immobilized at equal molarity (Fig. 4A). We chose IL-5/Mpz sICs as NK cells do not express the IL-5 receptor. While MIP1-β responses were comparable between the two triggers,

degranulation (CD107a) and TNFα responses showed a trend towards lower activation by sICs compared to immobilized IgG (Mpz). Strikingly, IFNγ responses were significantly weaker when NK cells were incubated with sICs compared to immobilized IgG. In order to confirm this hierarchy of responses and to enhance the overall low activation by Fcγ compared to the PMA control, we changed the IC setup by generating reverse-orientation sICs consisting of human FcγR-specific mouse mAbs and goat-anti-mouse IgG $F(ab)_2$ fragments. NK cell activation by reverse sICs was compared to NK cell activation by immobilized FcγR specific mAbs (Fig. 4B). Here, we not only confirm our previous observations regarding MIP-1β and IFNγ, but we also confirm significantly lower TNFα and CD107a responses towards soluble complexes compared to immobilized mAbs. Importantly, these experiments validate that sICs readily activate primary NK cells and induce immunological effector functions. As in roughly 10% of the population NK cells express FcγRIIC (*49-52*), we also tested if this receptor plays a role in our measurements. Using the same three donors and an FcγRII specific mAb as described above, we did not observe an FcγRII-mediated response. Accordingly, we conclude that FcγRIIC expression did not play a role in our experiments (Fig. 4C). Taken together, we show that multivalent but not dimeric soluble immune complexes govern primary NK cell response and FcγRIIIA activation (Fig. 2A).

Measurement of FcγR activation in response to changing sIC size

We observed that the dimeric sIC CD20:Rtx molecule complex completely failed to trigger FcγRs, while potentially larger sICs based on multimeric antigens showed an efficient dose-dependent FcγR activation. In order to determine whether BW5147 FcγR-ζ reporter cells are able to respond to changes in sIC size, we tested cross-titrated amounts of antibody (mAb, infliximab, Ifx) and antigen (Ag, rhTNFα). To this end, the reporter cells were incubated with sIC of different mAb:Ag ratios by fixing one parameter and titrating the other. According to

the Heidelberger-Kendall precipitation curve (*12*) describing sIC size as being dependent on the mAb:Ag ratio, this should result in varying sIC sizes as an excess of either antigen or antibody results in the formation of smaller complexes compared to the large molecular complexes formed at around equal molarity. Changes in sIC size due to a varying mAb:Ag ratio were quantified using asymmetrical flow-field flow fractionation (AF4) (Fig. 5A and Table S1). Fig. S2 shows a complete run of such an analysis. AF4 analysis identifies the highest sIC mean molecular being approximately 2130 kDa at a 1:3 ratio (mAb Ifx : Ag TNF-α) with sICs getting smaller with increasing excess of either antigen or antibody, recapitulating a Heidelberger-Kendall-like curve. Incubation of the FcγR reporter cells with ICs of varying size indeed shows that the assay is sensitive to exactly monitor changes in sIC size (Fig. 5B). Accordingly, both FcγR types showed the strongest responses at mAb:Ag ratios of approximately 1:3. We then set out to test the accuracy of our reporter cell assay as a surrogate for primary human immune cells expressing FcγRs. To this end, we tested primary NK cells from three individual donors and measured NK cell MIP1-β upregulation in response to synthetic sICs of varying size and composition again using a similar assay setup optimized for NK cell activation. We chose MIP-1β upregulation as a cell surface marker to measure NK cell activation as it showed the highest responsiveness in previous experiments (Fig. 4). We could observe that primary immune cells expressing FcγRIIIA respond to IC size, confirming our assay to be an accurate surrogate for primary immune cell responses to soluble ICs (Fig. 5C). Convincingly, NK cell responses to sICs generated from trimeric antigen (rhTNFα) peaked at a different mAb:Ag ratio compared to NK cell responses to sICs generated from dimeric antigens (rhIL-5 and rhVEGFA). Of note, TNFα and VEGFA activate resting NK cells thus leading to higher MIP1-β positivity when NK cells are incubated in the presence of excess antigen. As NK cells do not express IL-5 receptor, this effect is not observed in the presence of excess IL-5. Regarding TNFα, NK cells still show a stronger activation by sICs generated under optimal mAb:Ag ratios compared to conditions where

232 excess antigen is used. The data reveal a direct correlation between sIC size and effector
233 responses. Conversely, when changing antibody concentrations using fixed amounts of
234 antigen, a consistent reduction of NK cell activation is observed in the presence of excess IgG
235 for all three mAb/Ag pairs.
236
237 *Quantification of sIC bioactivity in sera of SLE patients*
238 In order to apply the assay to a clinically relevant condition associated with the occurrence of
239 sICs we measured circulating sICs present in the serum of SLE patients with variable disease
240 activity. Sera from 4 healthy donors and 25 SLE patients were investigated for FcγRIIIA and
241 FcγRIIB/C activation. Reporter cells readily produced IL-2 in response to patient sera in a
242 dose-dependent manner (shown exemplarily for some SLE patients, see Fig. 6A), which was
243 not the case when sera from healthy controls were tested. Consistent with the observation that
244 FcγRI and FcγRIIA do not respond to synthetic sICs, reporter cells expressing these receptors
245 did also not respond to the tested serum samples (Fig. 6A, lower panel). While this reaction
246 pattern already indicated that sICs are the reactive component measured in SLE patients' sera,
247 we further demonstrate that FcγRIIIA and FcγRIIB/C activation depends on the presence of
248 serum ICs by analyzing patient serum before and after polyethylene glycol (PEG)
249 precipitation and depletion of sICs (Fig. 6B). Next, we calculated the area under the curve
250 (AUC) values for all 25 SLE patient titrations and normalized them to the AUC values
251 measured for healthy individuals. The resulting index values were then correlated with
252 established biomarkers of SLE disease activity, such as anti-dsDNA titers (α-dsDNA) and
253 concentrations of the complement cleavage product C3d (Fig. 6C). We observed a significant
254 correlation between our FcγRIIIA activation index values and both of the determined disease
255 activity markers, anti-dsDNA titers and C3d concentration ($p=0.0465$ and $p=0.0052$,
256 respectively). FcγRIIB/C on the other hand showed no significant correlation with either
257 biomarker. We assume these interrelations may be due to the influence of IgG sialyation

found to be reduced in active SLE (*53*). Generally, de-sialylation of IgG leads to stronger binding by the activating receptors FcγRI, FcγRIIA and FcγRIII while it reduces the binding affinity of the inhibitory FcγRIIB (*54*). In sum, our assay allows the indirect quantification of clinically relevant sICs in sera of SLE patients.

Assay application to clinically relevant in vivo lupus and arthritis mouse models

BW5147 reporter cells stably expressing chimeric mouse as well as rhesus macaque FcγRs have already been generated using the here described methodology and were successfully used to measure FcγR activation by opsonized adherent cells in previous studies (*47, 55*) (mFcγR reporter cells). As the human FcγR reporter cells described here are sensitive to certain sICs, we next aimed to translate the assay to clinically relevant animal models. To this end, we incubated previously described FcγR reporter cells expressing chimeric mouse FcγRs (*47*) with sera from lupus (NZB/WF1) or arthritis (K/BxN) mice with active autoimmune disease. The reporter assay was performed as described above. We chose to measure the stimulation of the activating receptors, mFcγRIII and mFcγRIV, that correspond to human FcγRIII and show a similar cellular distribution and immune function (*16*). Incubation with synthetic sICs generated from rhTNFα and mouse-anti-hTNFα IgG1 showed both of the mFcγR reporter cells to be equally responsive to sICs (Fig. 7A). Parental BW5147 cells expressing no FcγRs served as a control. The sera of three mice per group were analysed and compared to sera from wildtype C57BL/6 mice, which served as a healthy control. C57BL/6 mice were chosen, as healthy K/BxN or NZB/WF1 mice cannot be reliably defined. This is due to the unpredictable disease progression in these mouse models starting from a young age. We consistently detected mFcγR activation by sera from K/BxN or NZB/WF1 compared to C57BL6 mice (Fig. 7B). While the mFcγRIII responses were generally high and similar between K/BxN and NZB/WF1 mice, mFcγRIV responsiveness attended to be lower and individually more variable. Altogether, the assay enables the reliable detection of sICs in sera

of mice with immune-complex mediated diseases making it a promising novel tool to monitor sICs as a biomarker of disease activity.

Discussion

In this study we established, validated and applied a new assay system that is able for the first time to selectively detect soluble multimeric immune complexes as discrete ligands of FcγR. Major findings are i) that sICs cross-link and trigger human FcγRs IIB/C and IIIA but are neglected by activating FcγRI and IIA; ii) that sICs potency is strictly stoichiometry- and size-dependent and thus reproducing the classical Heidelberger-Kendall curve iii) that the overall functional design of FcγRs is adapted to physical cross-linking by soluble vs. membrane-bound immune complexes. The new test system has various obvious applications in medicine and pharmacy.

A novel assay for the quantification of disease-associated as well as synthetic sICs

The new approach presents an important and implementable advancement in immunological methodology as it enables the sensitive detection of receptor-activating ICs by a relatively simple, scalable *in vitro* bioassay with high-throughput potential. Based on our pilot study demonstrating that the sIC-mediated FcγRIIIA activation correlated with SLE disease markers, this is of great value for larger prospective clinical studies in patients with autoimmune diseases such as systemic lupus erythematosus (SLE) and rheumatoid arthritis (RA), where circulating ICs have long been shown to crucially contribute to tissue damage and disease manifestations (*40, 41, 56-58*). Disease-associated, endogenous sICs can also occur during infection, e.g. generated after antibody-mediated destruction of pathogenic viruses or microbes or probably more likely due to the oligomeric nature of numerous viral and bacterial structural proteins generated e.g. by SARS-CoV2 (*59-61*) HIV and hepatitis B virus (HBV) infection, during which circulating sICs are generated (*37, 62*). As the assay also

enables the sensitive and quantitative measurement of FcγR ligand bioactivity it allows the detection of sICs not only in clinical specimens but also pharmaceutical preparations of IgG and Fc-fusion proteins for therapeutic use (*46*). The presence of ICs in therapeutic preparations or sIC formation following patient treatment is unwanted due to the risk of side effects such as lupus-like syndrome which has been linked to mAb treatment in patients receiving infliximab (*63*) or bevacizumab (*64*), both mAbs used in this study. As this assay is highly sensitive to any aggregation of IgG, it also represents a tool to control the purity, quality and stability of mAb preparations produced for therapeutic use in patients. In addition, the assessment of sIC-mediated FcγR activation allows for optimization of mAbs and Fc-fusion proteins regarding their molecular design and manufacturing. Specifically, Fc-molecules targeting cytokines and soluble factors, which result in sIC formation, could be designed for reduced or enhanced FcγR activation such as glyco-engineered mAbs or LALA-mutant mAbs (*65, 66*). Notably, the scalability of this cell-based test system does allow for large-scale screening of samples.

sICs form FcγR ligands with distinct functional profiles

While immobilized ICs decorating infected cells, viral particles or microbial surfaces restrict their triggering effect to a single immune cell residing in very close vicinity, sICs can rapidly disseminate reaching a high number of immune effector cells thus developing a systemic effect with far reaching and long-lasting or even threatening consequences for the host as a whole. This could explain the very tight control of sIC governed effector programs and the unresponsiveness of activating receptors like FcγRI and IIA. We also observed a difference in the response patterns for FcγRIIIA and FcγRII/B/C depending on the solubility of clustered IgG (immobilized versus soluble ICs) which we validated for FcγRIIIA using primary human NK cells (Fig. 4 and 5C). Importantly,only multimeric but not dimeric sICs can trigger FcγR activation. This highlights the fundamental structural influence of the particular antigen as

well as the IgG molecule on sIC dimension and subsequent FcγR-mediated signal processing. The ability of the here described assay to define and quantify the activation of individual FcγRs by sIC ligands is not achievable using primary immune cells due to redundant immune responses upon FcγR activation and complex, overlapping expression pattern of FcγRs. Finally, and in contrast to primary human cells, murine BW5147 reporter cells are largely inert to human cytokines, which provides a key advantage to measure FcγR activation selectively in human samples. Notably, the two basically sIC-responsive human FcγR types, i.e. FcγRIIIA and FcγRIIB, are either highly activating versus strongly inhibitory and thus show a mutually exclusive expression pattern (ref. review, z.B. Ravetch und Falk). FcγRIIIA mediates ADCC elicited by NK cells and the induction of a pro-inflammatory cytokine profile by $CD16^{+}$ monocytes, while FcγRIIIB is a GPI-anchored receptor on neutrophils. FcγRIIB is an inhibitory receptor expressed by B cells and dendritic cells (DCs) regulating B cell activation, antibody production by plasma cells and the activation state of DCs, while the activating FcγRIIC is found on NK cells mediating ADCC. However, as FcγRIIC is only expressed by roughly 10% of the human population, its role is still poorly understood (*49-52*). Given the here shown fundamental difference in FcγR reactivity towards multimeric sICs versus immobilized IgG it is tempting to speculate that FcγRIIIA- and FcγRIIB/C-positive immune cells might have evolved to differentially perceive these different FcγR ligands (sICs versus membrane bound insoluble ICs) and translate them into distinct reaction patterns. This could be achieved by differences in receptor density, signal transduction or regulation of receptor expression. Consulting the literature indeed supports our hypothesis with neutrophils, B cells and NK cells being efficiently activated by sICs via almost identical receptor ectodomains (*18, 28, 67, 68*), while the immunological outcome of their triggering very much differs.

Dynamic sIC size measurement and monitoring of bioactivity in sIC-associated diseases

We provide for the first time a simultaneous functional and biophysical assessment of the paradigmatic Heidelberger-Kendall precipitation curve (*12, 13*). While previous work already revealed that large and small sICs differentially impacts IL-6 production in PBMCs (*6*), the dynamics of FcγR activation resulting from constant changes in sIC size have not been explored on a systematic basis. This was undertaken in this study by directly analyzing synthetic ICsformed by highly pure recombinant components via AF4 (Fig. 5A, Fig. S2, Table S1). Our data document that sIC size is indeed governed by antibody:antigen ratios covering a wide range of sizes up to several megadaltons. In the presence of increasing amounts of antibody or antigen deviating from an optimal antibody:ratio, sIC size steadily decreases. Further, by the measurement of FcγR activation we now translate sIC size directly to asimple but precise read-out. In doing so, we show that sIC size essentially tunes FcγR activation on and off. Thus, our new test system can not only contribute to the functional detection and quantification of clinically relevant sICs but also provides a starting point on how to avoid pathological consequences by influencing the sIC size, for example by administering therapeutic antibodies or recombinant antigens in optimized concentrations, thus becoming relevant in clinical pharmacokinetics.

Limitations of the reporter system and conclusions

While it is known that FcγRIIA requires FcγRIIIB or FcRn to efficiently respond to ICs (*22, 23, 69*), unexpectedly, we found that FcγRI is not activated by sICs in our assay. We assume that FcγRI interaction with sICs might require a native cellular environment given that a major function of this FcγR is the uptake and processing of antigen via ICs even in the absence of a signaling motif (*21*). However, we find that FcγRI ectodomains alone are not responsive to sICs implying a thoroughly different cross-linking threshold for FcγRI

compared with FcγRIIB and IIIA. This feature is possibly linked to its molecular architecture being the only high-affinity FcγR with three extracellular Ig domains compared to the two domains found in other FcγRs with lower affinity to monomeric IgG. This observation also reflects a general consideration regarding the BW5147 reporter system. While providing a robust and uniform read-out using a scalable cell-based approach, the assay is not able to reflect native immune cell functions governed by cell-intrinsic signalling cascades. The major advancements of this reporter system include i) a higher accuracy regarding FcγR activation compared to merely affinity measurements, ii) an sIC size dependent quantification of FcγR responsiveness and iii) the identification of FcγR activating sICs in autoimmunity and infection. Finally, this scalable, sensitive and robust system to detect FcγR activating sICs in clinical samples might enable their identification in diseases that have not been linked to sIC-mediated pathology, yet.

Materials and Methods

Cell culture: All cells were cultured in a 5% CO_2 atmosphere at 37°C. BW5147 mouse thymoma cells (BW, obtained from ATCC: TIB-47) were maintained at $3x10^5$ to $9x10^5$ cells/ml in Roswell Park Memorial Institute medium (RPMI GlutaMAX, Gibco) supplemented with 10% (vol/vol) fetal calf serum (FCS, Biochrom), sodium pyruvate (1x, Gibco) and β-mercaptoethanol (0.1 mM, Gibco). 293T-CD20 (kindly provided by Irvin Chen, UCLA (*70*)) were maintained in Dulbecco's modified Eagle's medium (DMEM, Gibco) supplemented with 10% (vol/vol) FCS.

FcγR receptor activation assay: FcγR activation was measured adapting a previously described cell-based assay (*45, 71*). The assay was modified to measure FcγR activation in solution. Briefly, $2x10^5$ mouse BW-FcγR (BW5147) reporter cells were incubated with

414 synthetic sICs or diluted serum in a total volume of 100 µl for 16 h at 37°C and 5% CO_2.
415 Incubation was performed in a 96-well ELISA plate (Nunc maxisorp) pre-treated with
416 PBS/10% FCS (v/v) for 1 h at 4°C. Immobilized IgG was incubated in PBS on the plates prior
417 to PBS/10% FCS treatment. Reporter cell mIL-2 secretion was quantified via ELISA as
418 described (*45*).
419
420 *Recombinant antigens and monoclonal antibodies to form sICs:* Recombinant human (rh)
421 cytokines TNF, IL-5, and VEGFA were obtained from Stem Cell technologies. Recombinant
422 CD20 was obtained as a peptide (aa141-188) containing the binding region of rituximab
423 (Creative Biolabs). FcγR-specific mAbs were obtained from Stem Cell technologies (CD16:
424 clone 3G8; CD32: IV.3). Reverse sICs were generated from these receptor-specific antibodies
425 using goat-anti-mouse IgG $F(ab)_2$ fragments (Invitrogen) in a 1:1 ratio. Pharmaceutically
426 produced humanized monoclonal IgG1 antibodies infliximab (Ifx), bevacizumab (Bvz),
427 mepolizumab (Mpz) and rituximab (Rtx) were obtained from the University Hospital
428 Pharmacy Freiburg. Mouse anti-hTNFα (IgG2b, R&D Systems, 983003) was used to generate
429 sICs reactive with mouse FcγRs. sICs were generated by incubation of antigens and
430 antibodies in reporter cell medium or PBS for 2 h at 37°C.
431
432 *Lentiviral transduction:* Lentiviral transduction of BW5147 cells was performed as described
433 previously (*47, 55*). In brief, chimeric FcγR-CD3ζ constructs (*45*) were cloned into a
434 pUC2CL6IPwo plasmid backbone. For every construct, one 10-cm dish of packaging cell line
435 at roughly 70% density was transfected with the target construct and two supplementing
436 vectors providing the VSV gag/pol and VSV-G-env proteins (6 µg of DNA each) using
437 polyethylenimine (22.5 µg/ml, Sigma) and Polybrene (4 µg/ml; Merck Millipore) in a total
438 volume of 7 ml (2 ml of a 15-min-preincubated transfection mix in serum-free DMEM added
439 to 5 ml of fresh full DMEM). After a medium change, virus supernatant harvested from the

packaging cell line 2 days after transfection was then incubated with target BW cells overnight (3.5 ml of supernatant on 10^6 target cells), followed by expansion and pool selection using complete medium supplemented with 2 µg/ml of puromycin (Sigma) over a one week culture period.

BW5147 toxicity test: Cell counting was performed using a Countess II (Life Technologies) according to supplier instructions. Cell toxicity was measured as a ratio between live and dead cells judged by trypan blue staining over a 16 h time frame in a 96well format (100 µl volume per well). BW5147 cells were mixed 1:1 with Trypan blue (Invitrogen) and analysed using a Countess II. rhTNFα was diluted in complete medium.

human IgG suspension ELISA: 1 µg of IgG1 (rituximab in PBS, 50 µl/well) per well was incubated on a 96well microtiter plate (NUNC Maxisorp) pre-treated (2h at RT) with PBS supplemented with varying percentages (v/v) of FCS (PAN Biotech). IgG1 bound to the plates was detected using an HRP-conjugated mouse-anti-human IgG mAb (Jackson ImmunoResearch).

BW5147 cell flow cytometry: BW5147 cells were harvested by centrifugation at 900 g and RT from the suspension culture. $1x10^6$ cells were stained with PE- or FITC-conjugated anti-human FcγR mAbs (BD) or a PE-TexasRed-conjugated human IgG-Fc fragment (Rockland) for 1h at 4°C in PBS/3%FCS. After 3 washing steps in PBS/3%FCS, the cells were transferred to Flow cytometry tubes (BD) and analysed using BD LSR Fortessa and FlowJo (V10) software.

NK cell activation flow cytometry: PBMC were purified from donor blood using Lymphocyte separation Media (Anprotec). Primary NK cells were separated from donor PBMCs via

magnetic bead negative selection (Stem Cell technologies) and NK cell purity was confirmed via staining of CD3 (Biolegend, clone HIT3a), CD16 (Biolegend, clone 3G8) and CD56 (Miltenyi Biotec, clone AF12-7H3). 96well ELISA plates (Nunc Maxisorp) were pre-treated with PBS/10% FCS (v/v) for 1 h at 4°C. NK cells were stimulated in pre-treated plates and incubated at 37°C and 5% CO_2 for 4 h. Golgi Plug and Golgi Stop solutions (BD) were added as suggested by supplier. CD107a (APC, BD, H4A3) specific conjugated mAb was added at the beginning of the incubation period. Following the stimulation period, MIP-1β (PE, BD Pharmigen), IFNγ (BV-510, Biolegends, 4SB3) and TNFα (PE/Cy7, Biolegends, MAB11) production was measured via intracellular staining Cytokines (BD, CytoFix/CytoPerm, Kit as suggested by the supplier). 50 ng/ml PMA (InvivoGen) + 0.5 µM Ionomycin (InvivoGen) were used as a positive stimulation control for NK cell activation. After 3 washing steps in PBS/3%FCS, the cells were transferred to Flow cytometry tubes (BD) and analysed using a BD FACS Fortessa and FlowJo (V10) software. FcγRII or FcγRIII block was performed by addition of receptor specific mAbs (Stem cell technologies, IV.3 and 3G8) at a 1:100 dilution at the beginning of the incubation period. Cells were transferred to Flow cytometry tubes (BD) and analyzed using BD LSR Fortessa and FlowJo (V10) software.

Asymmetric flow field flow fractionation (AF4): The AF4 system consisted of a flow controller (Eclipse AF4, Wyatt), a MALS detector (DAWN Heleos II, Wyatt), a UV detector (1260 Infinity G1314F, Agilent) and the separation channel (SC channel, PES membrane, cut-off 10 kDa, 490 µm spacer, wide type, Wyatt). Elution buffer: 1.15 g/L Na_2HPO_4 (Merck), 0.20 g/L NaH_2PO_4 x H_2O (Merck), 8.00 g/L NaCl (Sigma) and 0,20 g/L NaN_3 (Sigma), adjusted to pH 7.4, filtered through 0.1 µm. AF4 sequence (Vx = cross flow in mL/min): (a) elution (2 min, Vx: 1.0); (b) focus (1 min, Vx: 1.0), focus + inject (1 min, Vx: 1.0, inject flow: 0.2 mL/min), repeated three times; (c) elution (30 min, linear Vx gradient: 1.0 to 0.0); (d) elution (15 min, Vx: 0.0); (e) elution + inject (5 min, Vx: 0.0). A total protein mass of 17±0.3

µg (Ifx, rhTNFα or ICs, respectively) was injected. The eluted sample concentration was calculated from the UV signal at 280 nm using extinction coefficients of 1.240 mL/(mg cm) or 1.450 mL/(mg cm) in the case of TNFα or Ifx, respectively. For the ICs, extinction coefficients were not available and difficult to calculate as the exact stoichiometry is not known. An extinction coefficient of 1.450 mL/(mg cm) was used for calculating the molar masses of all ICs. Especially in the case of ICs rich in TNFα, the true coefficients should be lower, and the molar masses of these complexes are overestimated by not more than 14 %. The determined molar masses for TNFα-rich complexes are therefore biased but the observed variations in molar mass for the different ICs remain valid. The mass-weighted mean of the distribution of molar masses for each sample was calculated using the ASTRA 7 software package (Wyatt).

SLE patient cohort: Sera from patients with SLE were obtained from the Immunologic, Rheumatologic Biobank (IR-B) of the Department of Rheumatology and Clinical Immunology. Biobanking and the project were approved by the local ethical committee of the University of Freiburg (votes 507/16 and 624/14). All patients who provided blood to the biobank had provided written informed consent. Ethical Statement: The study was designed in accordance with the guidelines of the Declaration of Helsinki (revised 2013). Patients with SLE (n = 25) and healthy controls (n = 4) were examined. All patients met the revised ACR classification criteria for SLE. Disease activity was assessed using the SLEDAI-2K score. C3d levels were analyzed in EDTA plasma using rocket double decker immune-electrophoresis with antisera against C3d (Polyclonal Rabbit Anti-Human C3d Complement, Agilent) and C3c (Polyclonal Rabbit Anti-Human C3c Complement Agilent) as previously described (*72*). Anti-human dsDNA antibodies titers were determined in serum using an anti-dsDNA IgG ELISA kit (diagnostik-a GmbH).

518 *Patient serum IC precipitation:* For polyethylene glycol (PEG) precipitation human sera were
519 mixed with PEG 6000 (Sigma-Aldrich) in PBS at a final concentration of 10% PEG 6000.
520 After overnight incubation at 4°C, ICs were precipitated by centrifugation at 2000 x g for
521 30 min at 4 °C, pellets were washed once with PEG 6000 and then centrifugated at 2000 x g
522 for 20 min at 4 °C. Supernatants were harvested and precipitates re-suspended in pre-warmed
523 PBS for 1 h at 37 °C. IgG concentrations of serum, precipitates and supernatants obtained
524 after precipitation were quantified by Nanodrop (Thermo Scientific™) measurement.
525
526 *Mice and Models:* Animal experiments were approved by the local governmental commission
527 for animal protection of Freiburg (Regierungspräsidium Freiburg, approval no. G16/59 and
528 G19/21). Lupus-prone (NZBxNZW)F1 mice (NZB/WF1) were generated by crossing
529 NZB/BlNJ mice with NZW/LacJ mice, purchased from The Jackson Laboratory. KRNtg mice
530 were obtained from F. Nimmerjahn (Universität Erlangen-Nürnberg) with the permission of
531 D. Mathis and C. Benoist (Harvard Medical School, Boston, MA), C57BL/6 mice (BL/6) and
532 NOD/ShiLtJArc (NOD/Lt) mice were obtained from the Charles River Laboratories. K/BxN
533 (KRNtgxNOD)F1 mice (K/BxN) were obtained by crossing KRNtg mice and NOD/Lt mice.
534 All mice were housed in a 12-h light/dark cycle, with food and water ad libitum. Mice were
535 euthanized and blood collected for serum preparation from 16 weeks old BL/6 animals, from
536 16 weeks old arthritic K/BxN animals and from 26 – 38 weeks old NZB/WF1 mice with
537 established glomerulonephritis.
538
539 *Statistical analyses:* Statistical analyses were performed using Graphpad Prism software (v6)
540 and appropriate tests.
541
542
543

Acknowledgements: We thank T. Schleyer (IR-B Biobank) for providing patient samples. We are indebted to Falk. Nimmerjahn (Universität Erlangen-Nürnberg) for providing KRNtg mice. **Funding:** This work was supported by an intramural junior investigator fund of the Faculty of Medicine to PK (EQUIP - Funding for Medical Scientists, Faculty of Medicine, University of Freiburg), by the German Research foundation (DFG) (FOR2830 HE 2526/9-1) and NaFoUniMedCovid19“ (FKZ: 01KX2021) – COVIM and FKZ 100493916 B-FAST to HH, by the DFG research grant TRR130 to REV and the Ministry of Science, Research, and Arts Baden-Württemberg (Margarete von Wrangell Programm) to NC. **Author contributions:** HC and PK designed and developed the reporter system, conducted Fc-gamma receptor activation experiments and prepared synthetic immune complexes. AMP, US and REV manage the SLE patient cohort, provided sera and performed immune complex precipitation as well as IgG quantification. MH designed and performed AF4 analyses. NC manages the mouse models and provided sera. HH and PK supervised all experiments. HC and PK analysed and interpreted data. PK wrote the paper assisted by HC, AMP, MH, NC, REV and HH. **Competing interests:** The authors declare no financial and non-financial competing interests. **Data and materials availability:** All data associated with this study are present in the paper or Supplementary Materials.

Supplementary Materials

Fig. S1. rhTNFα is not toxic to mouse lymphocyte BW5147 cells even at high concentrations.

Fig. S2. AF4 elution profiles of Ifx/TNFα-immune complexes.

Table S1. Analysis of the molar mass distribution of ICs from AF4 data.

References

1. L. L. Lu, T. J. Suscovich, S. M. Fortune, G. Alter, Beyond binding: antibody effector functions in infectious diseases. *Nat Rev Immunol* **18**, 46-61 (2018).
2. J. V. Ravetch, S. Bolland, IgG Fc receptors. *Annu Rev Immunol* **19**, 275-290 (2001).
3. C. E. van der Poel, R. M. Spaapen, J. G. van de Winkel, J. H. Leusen, Functional characteristics of the high affinity IgG receptor, FcgammaRI. *J Immunol* **186**, 2699-2704 (2011).
4. P. Bruhns *et al.*, Specificity and affinity of human Fcgamma receptors and their polymorphic variants for human IgG subclasses. *Blood* **113**, 3716-3725 (2009).
5. D. Urlaub *et al.*, Activation of natural killer cells by rituximab in granulomatosis with polyangiitis. *Arthritis Res Ther* **21**, 277 (2019).
6. A. Lux, X. Yu, C. N. Scanlan, F. Nimmerjahn, Impact of immune complex size and glycosylation on IgG binding to human FcgammaRs. *J Immunol* **190**, 4315-4323 (2013).
7. F. Kiefer *et al.*, The Syk protein tyrosine kinase is essential for Fc gamma receptor signaling in macrophages and neutrophils. *Mol Cell Biol* **18**, 4209-4220 (1998).
8. Y. Luo, J. W. Pollard, A. Casadevall, Fcgamma receptor cross-linking stimulates cell proliferation of macrophages via the ERK pathway. *J Biol Chem* **285**, 4232-4242 (2010).
9. S. Greenberg, P. Chang, S. C. Silverstein, Tyrosine phosphorylation of the gamma subunit of Fc gamma receptors, p72syk, and paxillin during Fc receptor-mediated phagocytosis in macrophages. *J Biol Chem* **269**, 3897-3902 (1994).
10. S. Bournazos, T. T. Wang, R. Dahan, J. Maamary, J. V. Ravetch, Signaling by Antibodies: Recent Progress. *Annu Rev Immunol* **35**, 285-311 (2017).
11. F. Nimmerjahn, J. V. Ravetch, Antibody-mediated modulation of immune responses. *Immunol Rev* **236**, 265-275 (2010).
12. M. Heidelberger, F. E. Kendall, A Quantitative Study of the Precipitin Reaction between Type Iii Pneumococcus Polysaccharide and Purified Homologous Antibody. *J Exp Med* **50**, 809-823 (1929).
13. M. Heidelberger, F. E. Kendall, The Precipitin Reaction between Type Iii Pneumococcus Polysaccharide and Homologous Antibody : Iii. A Quantitative Study and a Theory of the Reaction Mechanism. *J Exp Med* **61**, 563-591 (1935).
14. A. M. Duchemin, L. K. Ernst, C. L. Anderson, Clustering of the High-Affinity Fc Receptor for Immunoglobulin-G (Fc-Gamma-Ri) Results in Phosphorylation of Its Associated Gamma-Chain. *J Biol Chem* **269**, 12111-12117 (1994).
15. A. Getahun, J. C. Cambier, Of ITIMs, ITAMs, and ITAMis: revisiting immunoglobulin Fc receptor signaling. *Immunol Rev* **268**, 66-73 (2015).
16. P. Bruhns, F. Jonsson, Mouse and human FcR effector functions. *Immunol Rev* **268**, 25-51 (2015).
17. P. Bruhns, Properties of mouse and human IgG receptors and their contribution to disease models. *Blood* **119**, 5640-5649 (2012).
18. F. Nimmerjahn, J. V. Ravetch, Fcgamma receptors as regulators of immune responses. *Nat Rev Immunol* **8**, 34-47 (2008).
19. F. Nimmerjahn, J. V. Ravetch, Fcgamma receptors: old friends and new family members. *Immunity* **24**, 19-28 (2006).
20. M. Guilliams, P. Bruhns, Y. Saeys, H. Hammad, B. N. Lambrecht, The function of Fcgamma receptors in dendritic cells and macrophages. *Nat Rev Immunol* **14**, 94-108 (2014).
21. Z. K. Indik *et al.*, The high affinity Fc gamma receptor (CD64) induces phagocytosis in the absence of its cytoplasmic domain: the gamma subunit of Fc gamma RIIIA imparts phagocytic function to Fc gamma RI. *Exp Hematol* **22**, 599-606 (1994).
22. G. Fossati, R. C. Bucknall, S. W. Edwards, Insoluble and soluble immune complexes activate neutrophils by distinct activation mechanisms: changes in functional responses induced by priming with cytokines. *Ann Rheum Dis* **61**, 13-19 (2002).

23. J. J. Hubbard *et al.*, FcRn is a CD32a coreceptor that determines susceptibility to IgG immune complex-driven autoimmunity. *J Exp Med* **217**, (2020).
24. A. Pincetic *et al.*, Type I and type II Fc receptors regulate innate and adaptive immunity. *Nat Immunol* **15**, 707-716 (2014).
25. G. Vidarsson, G. Dekkers, T. Rispens, IgG subclasses and allotypes: from structure to effector functions. *Front Immunol* **5**, 520 (2014).
26. M. Z. Tay, K. Wiehe, J. Pollara, Antibody-Dependent Cellular Phagocytosis in Antiviral Immune Responses. *Front Immunol* **10**, 332 (2019).
27. E. A. Laborde *et al.*, Immune complexes inhibit differentiation, maturation, and function of human monocyte-derived dendritic cells. *J Immunol* **179**, 673-681 (2007).
28. S. Kang *et al.*, IgG-Immune Complexes Promote B Cell Memory by Inducing BAFF. *J Immunol* **196**, 196-206 (2016).
29. V. Granger, M. Peyneau, S. Chollet-Martin, L. de Chaisemartin, Neutrophil Extracellular Traps in Autoimmunity and Allergy: Immune Complexes at Work. *Front Immunol* **10**, 2824 (2019).
30. S. Berger, H. Ballo, H. J. Stutte, Immune complex-induced interleukin-6, interleukin-10 and prostaglandin secretion by human monocytes: A network of pro- and anti-inflammatory cytokines dependent on the antigen:antibody ratio. *Eur J Immunol* **26**, 1297-1301 (1996).
31. L. Koenderman, Inside-Out Control of Fc-Receptors. *Front Immunol* **10**, 544 (2019).
32. R. Plomp *et al.*, Subclass-specific IgG glycosylation is associated with markers of inflammation and metabolic health. *Sci Rep* **7**, 12325 (2017).
33. T. C. Pierson *et al.*, The stoichiometry of antibody-mediated neutralization and enhancement of West Nile virus infection. *Cell Host Microbe* **1**, 135-145 (2007).
34. K. R. Patel, J. T. Roberts, A. W. Barb, Multiple Variables at the Leukocyte Cell Surface Impact Fc gamma Receptor-Dependent Mechanisms. *Front Immunol* **10**, 223 (2019).
35. S. Bohm, D. Kao, F. Nimmerjahn, Sweet and sour: the role of glycosylation for the anti-inflammatory activity of immunoglobulin G. *Current topics in microbiology and immunology* **382**, 393-417 (2014).
36. R. J. Stopforth *et al.*, Detection of Experimental and Clinical Immune Complexes by Measuring SHIP-1 Recruitment to the Inhibitory FcgammaRIIB. *J Immunol* **200**, 1937-1950 (2018).
37. T. T. Wang, J. V. Ravetch, Immune complexes: not just an innocent bystander in chronic viral infection. *Immunity* **42**, 213-215 (2015).
38. D. H. Yamada *et al.*, Suppression of Fcgamma-receptor-mediated antibody effector function during persistent viral infection. *Immunity* **42**, 379-390 (2015).
39. U. Antes, H. P. Heinz, D. Schultz, D. Brackertz, M. Loos, C1q-bearing immune complexes detected by a monoclonal antibody to human C1q in rheumatoid arthritis sera and synovial fluids. *Rheumatol Int* **10**, 245-250 (1991).
40. R. H. Zubler *et al.*, Circulating and intra-articular immune complexes in patients with rheumatoid arthritis. Correlation of 125I-Clq binding activity with clinical and biological features of the disease. *J Clin Invest* **57**, 1308-1319 (1976).
41. D. Koffler, V. Agnello, R. Thoburn, H. G. Kunkel, Systemic lupus erythematosus: prototype of immune complex nephritis in man. *J Exp Med* **134**, 169-179 (1971).
42. T. V. Rajan, The Gell-Coombs classification of hypersensitivity reactions: a re-interpretation. *Trends in immunology* **24**, 376-379 (2003).
43. S. Tahir *et al.*, A CD153+CD4+ T follicular cell population with cell-senescence features plays a crucial role in lupus pathogenesis via osteopontin production. *J Immunol* **194**, 5725-5735 (2015).
44. A. Bano *et al.*, CD28 (null) CD4 T-cell expansions in autoimmune disease suggest a link with cytomegalovirus infection. *F1000Res* **8**, (2019).
45. E. Corrales-Aguilar *et al.*, A novel assay for detecting virus-specific antibodies triggering activation of Fcgamma receptors. *Journal of immunological methods* **387**, 21-35 (2013).

46. H. A. D. Lagasse, H. Hengel, B. Golding, Z. E. Sauna, Fc-Fusion Drugs Have FcgammaR/C1q Binding and Signaling Properties That May Affect Their Immunogenicity. *AAPS J* **21**, 62 (2019).
47. S. Van den Hoecke *et al.*, Hierarchical and Redundant Roles of Activating FcgammaRs in Protection against Influenza Disease by M2e-Specific IgG1 and IgG2a Antibodies. *J Virol* **91**, (2017).
48. M. Tanaka *et al.*, Activation of Fc gamma RI on monocytes triggers differentiation into immature dendritic cells that induce autoreactive T cell responses. *J Immunol* **183**, 2349-2355 (2009).
49. S. Lisi, M. Sisto, D. D. Lofrumento, S. D'Amore, M. D'Amore, Advances in the understanding of the Fc gamma receptors-mediated autoantibodies uptake. *Clin Exp Med* **11**, 1-10 (2011).
50. J. C. Anania, A. M. Chenoweth, B. D. Wines, P. M. Hogarth, The Human FcgammaRII (CD32) Family of Leukocyte FcR in Health and Disease. *Front Immunol* **10**, 464 (2019).
51. D. Metes *et al.*, Expression of functional CD32 molecules on human NK cells is determined by an allelic polymorphism of the FcgammaRIIC gene. *Blood* **91**, 2369-2380 (1998).
52. W. B. Breunis *et al.*, Copy number variation of the activating FCGR2C gene predisposes to idiopathic thrombocytopenic purpura. *Blood* **111**, 1029-1038 (2008).
53. F. Vuckovic *et al.*, Association of systemic lupus erythematosus with decreased immunosuppressive potential of the IgG glycome. *Arthritis Rheumatol* **67**, 2978-2989 (2015).
54. Y. Kaneko, F. Nimmerjahn, J. V. Ravetch, Anti-inflammatory activity of immunoglobulin G resulting from Fc sialylation. *Science* **313**, 670-673 (2006).
55. P. Kolb *et al.*, Identification and Functional Characterization of a Novel Fc Gamma-Binding Glycoprotein in Rhesus Cytomegalovirus. *J Virol* **93**, (2019).
56. U. E. Nydegger, J. S. t. Davis, Soluble immune complexes in human disease. *CRC Crit Rev Clin Lab Sci* **12**, 123-170 (1980).
57. R. J. Levinsky, J. S. Cameron, J. F. Soothill, Serum immune complexes and disease activity in lupus nephritis. *Lancet* **1**, 564-567 (1977).
58. R. J. Levinsky, Role of circulating soluble immune complexes in disease. *Arch Dis Child* **53**, 96-99 (1978).
59. L. Briant, N. Coudronniere, V. Robert-Hebmann, M. Benkirane, C. Devaux, Binding of HIV-1 virions or gp120-anti-gp120 immune complexes to HIV-1-infected quiescent peripheral blood mononuclear cells reveals latent infection. *J Immunol* **156**, 3994-4004 (1996).
60. S. K. Oh *et al.*, Identification of HIV-1 envelope glycoprotein in the serum of AIDS and ARC patients. *J Acquir Immune Defic Syndr (1988)* **5**, 251-256 (1992).
61. D. A. Vuitton, L. Vuitton, E. Seilles, P. Galanaud, A plea for the pathogenic role of immune complexes in severe Covid-19. *Clin Immunol* **217**, 108493 (2020).
62. K. Madalinski, B. Burczynska, K. H. Heermann, A. Uy, W. H. Gerlich, Analysis of viral proteins in circulating immune complexes from chronic carriers of hepatitis B virus. *Clin Exp Immunol* **84**, 493-500 (1991).
63. D. A. Wetter, M. D. Davis, Lupus-like syndrome attributable to anti-tumor necrosis factor alpha therapy in 14 patients during an 8-year period at Mayo Clinic. *Mayo Clin Proc* **84**, 979-984 (2009).
64. D. A. MacDonald *et al.*, Aflibercept exhibits VEGF binding stoichiometry distinct from bevacizumab and does not support formation of immune-like complexes. *Angiogenesis* **19**, 389-406 (2016).
65. K. O. Saunders, Conceptual Approaches to Modulating Antibody Effector Functions and Circulation Half-Life. *Front Immunol* **10**, 1296 (2019).
66. T. Li *et al.*, Modulating IgG effector function by Fc glycan engineering. *Proceedings of the National Academy of Sciences of the United States of America* **114**, 3485-3490 (2017).

67. M. R. Goodier *et al.*, Sustained Immune Complex-Mediated Reduction in CD16 Expression after Vaccination Regulates NK Cell Function. *Front Immunol* **7**, 384 (2016).
68. T. N. Mayadas, G. C. Tsokos, N. Tsuboi, Mechanisms of immune complex-mediated neutrophil recruitment and tissue injury. *Circulation* **120**, 2012-2024 (2009).
69. S. Nagarajan *et al.*, Cell-specific, activation-dependent regulation of neutrophil CD32A ligand-binding function. *Blood* **95**, 1069-1077 (2000).
70. K. Morizono *et al.*, Redirecting lentiviral vectors pseudotyped with Sindbis virus-derived envelope proteins to DC-SIGN by modification of N-linked glycans of envelope proteins. *J Virol* **84**, 6923-6934 (2010).
71. E. Corrales-Aguilar *et al.*, Human cytomegalovirus Fcgamma binding proteins gp34 and gp68 antagonize Fcgamma receptors I, II and III. *PLoS pathogens* **10**, e1004131 (2014).
72. E. Rother, B. Lang, R. Coldewey, K. Hartung, H. H. Peter, Complement split product C3d as an indicator of disease activity in systemic lupus erythematosus. *Clin Rheumatol* **12**, 31-35 (1993).

Figures

Figure 1

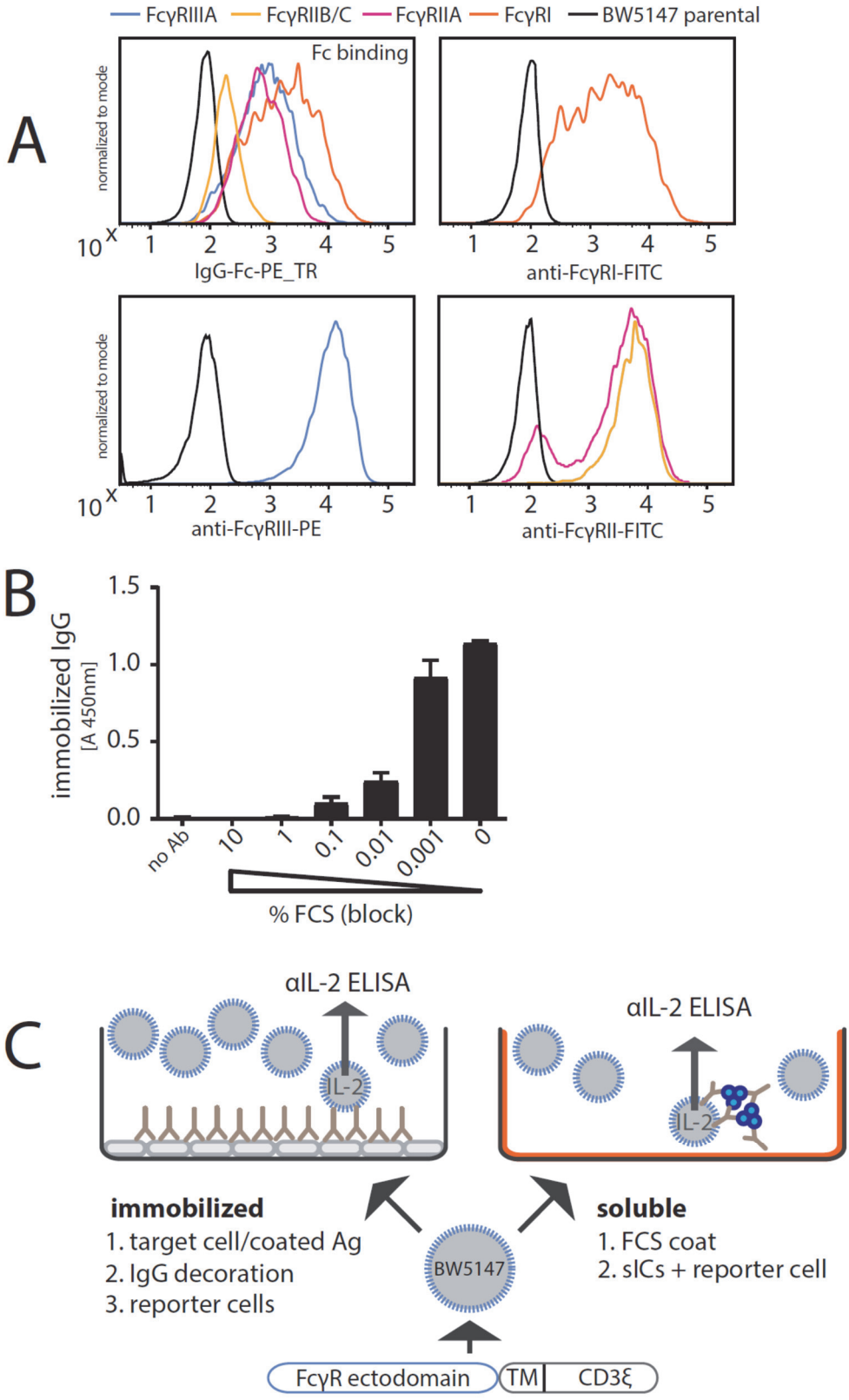

754

755 **Figure 2**

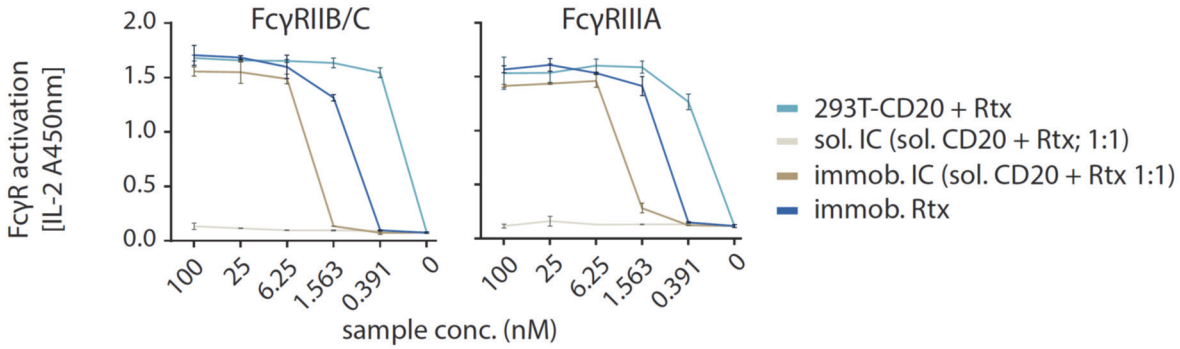

756

757 **Fig. 2. FcγRIIB/C and FcγRIIIA do not respond to small hetero-dimeric sICs but are**
758 **sensitive to immobilized IgG/ICs.** Dose-dependent activation of FcγR-bearing reporter cells
759 by immobilized IC can be mimicked by immobilized IgG. Response curves of human
760 FcγRIIB/C and FcγRIIIA are similar between opsonized cells (293T cells stably expressing
761 CD20 + Rtx), immobilized IC (rec. soluble CD20 + Rtx) and immobilized IgG (Rtx). sIC
762 formed by monovalent antigen (rec. soluble CD20) do not activate human FcγRs. X-Axis
763 shows sample concentration determined by antibody molarity. Y-Axis shows FcγR activation
764 determined by reporter cell IL-2 production.

765

766 **Figure 3**

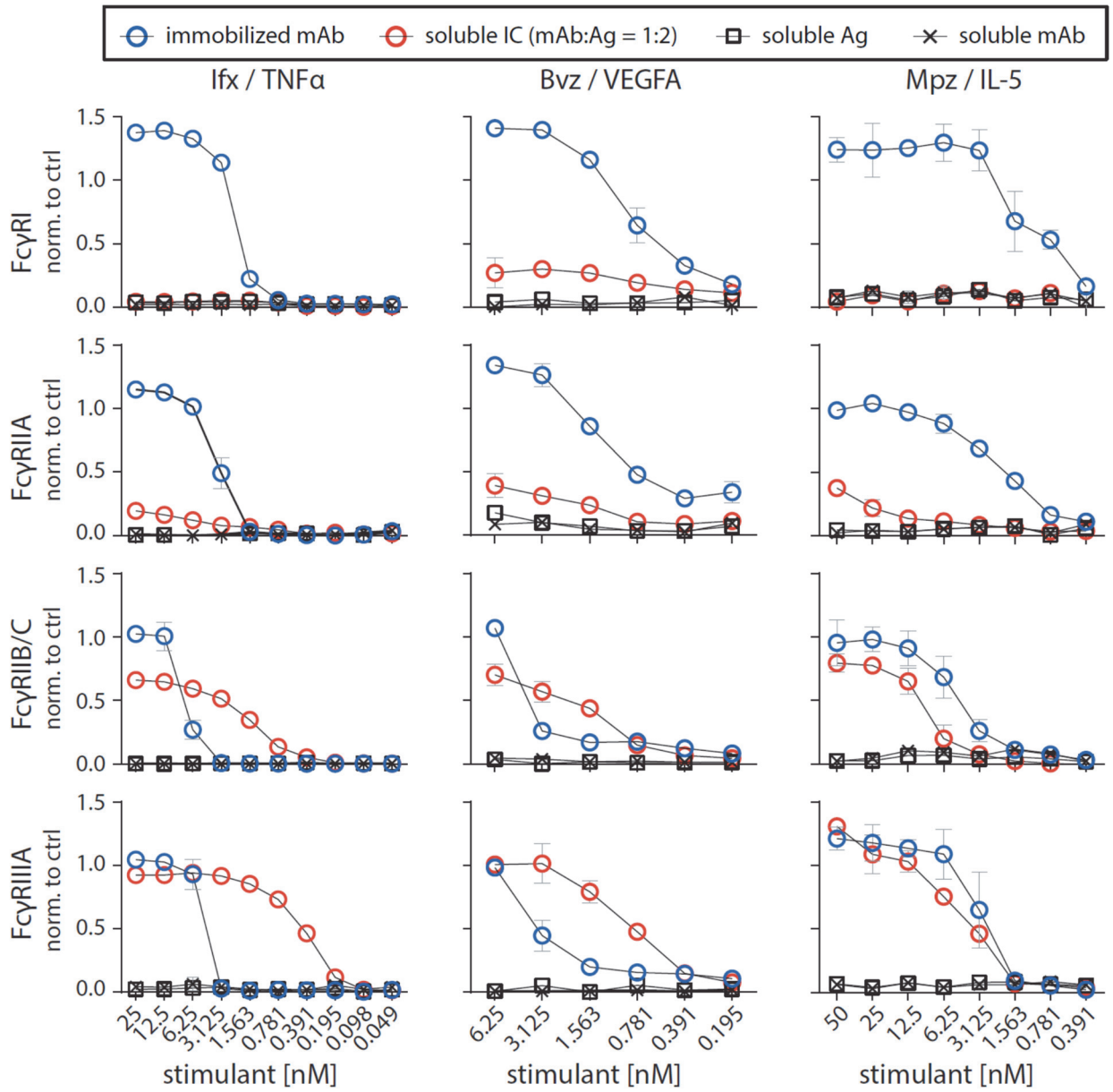

767
768

Fig. 3. FcγRIIB/C and FcγRIIIA are activated by sICs formed from multivalent antigens. Three different multivalent ultra-pure antigens (Ag) mixed with respective therapy-grade mAbs were used to generate sICs as indicated for each set of graphs (top to bottom). IC pairs: infliximab (Ifx) and rhTNFα; mepolizumab (Mpz) and rhIL-5; bevacizumab (Bvz) and rhVEGFA. X-Axis: concentrations of stimulant expressed as molarity of either mAb or Ag monomer and IC (expressed as mAb molarity) at a mAb:Ag ratio of 1:2. Soluble antigen or soluble antibody alone served as negative controls and were not sufficient to activate human FcγRs. FcγR responses were normalized to immobilized rituximab (Rtx) at 1µg/well (set to 1) and a medium control (set to 0). All FcγRs show dose-dependent activation towards immobilized IgG. FcγRIIA shows low activation at high sIC concentrations compared to immobilized IgG activation. FcγRI shows no activation towards sICs. FcγRIIIA and FcγRIIB/C are dose-dependently activated by sICs with responses comparable in strength to immobilized IgG stimulant. Experiments performed in technical replicates. Error bars = SD. Error bars smaller than symbols are not shown.

Figure 4

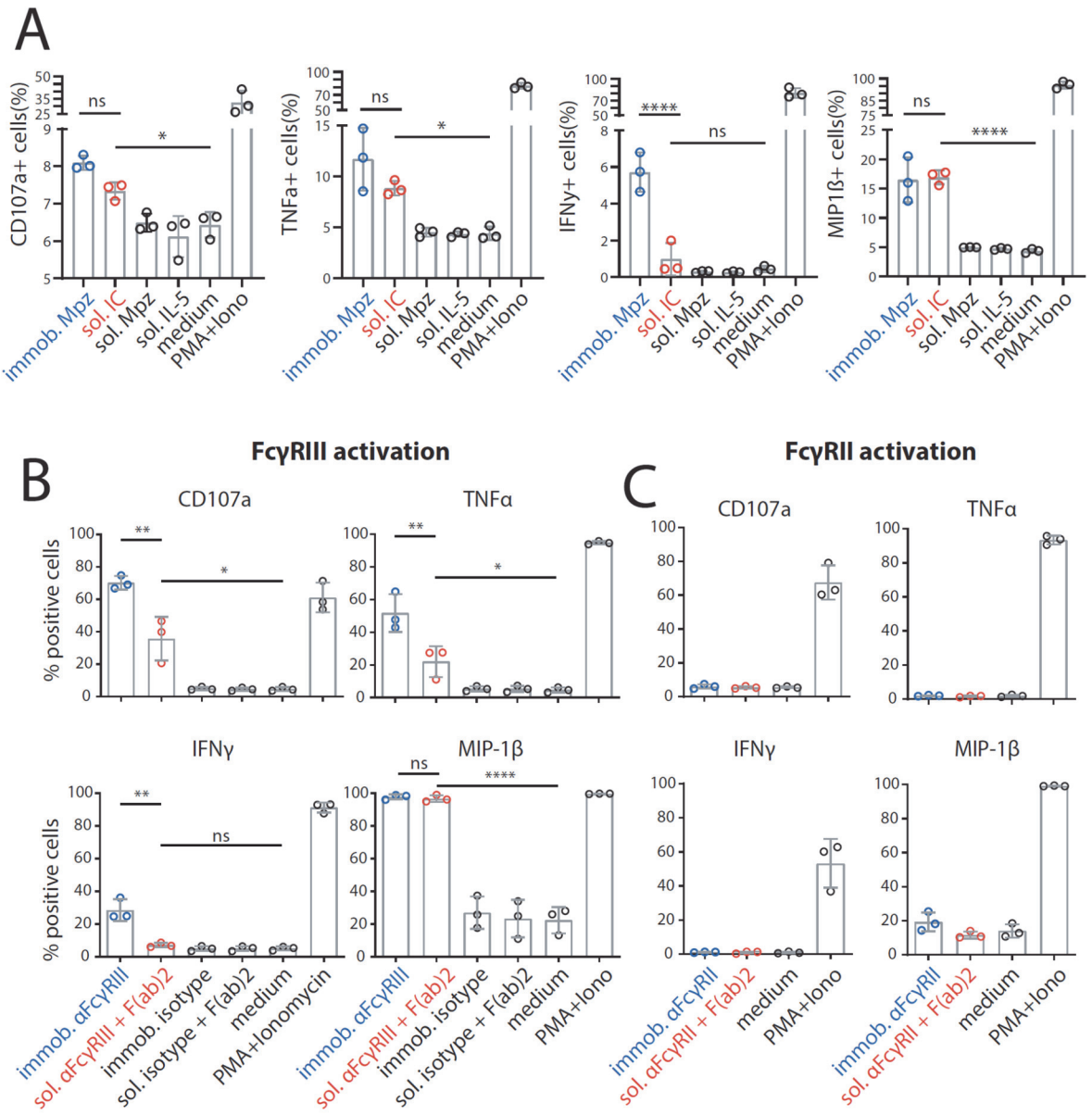

Fig. 4. The FcγRIII-dependent activation pattern of primary NK cells depends on IC solubility. Negatively selected primary NK cells purified from PBMCs of three healthy donors were tested for NK cell activation markers. Error bars = SD. Two-way ANOVA (Turkey). A) NK cells were incubated with immobilized IgG (mepolizumab, Mpz), soluble IC (Mpz:IL-5 = 1:1), soluble Mpz or soluble IL-5 (all at 200 nM, 10^6 cells). Incubation with PMA and Ionomycin (Iono) served as a positive control. Incubation with medium alone served as a negative control. B) NK cells were incubated for 4 h with immobilized FcγRIII-specific mAb, soluble mouse-anti-human IgG $F(ab)_2$ complexed FcγRIII-specific mAb (reverse sICs), immobilized IgG of non-FcγRIII-specificity (isotype control) or soluble $F(ab)_2$ complexed isotype control (all at 1µg, 10^6 cells). Incubation with PMA and Ionomycin served as a positive control. Incubation with medium alone served as a negative control. C) As in B using an FcγRII-specific mAb. NK cells from the tested donors in this study do not react to FcγRII activation.

802 **Figure 5**

803

804

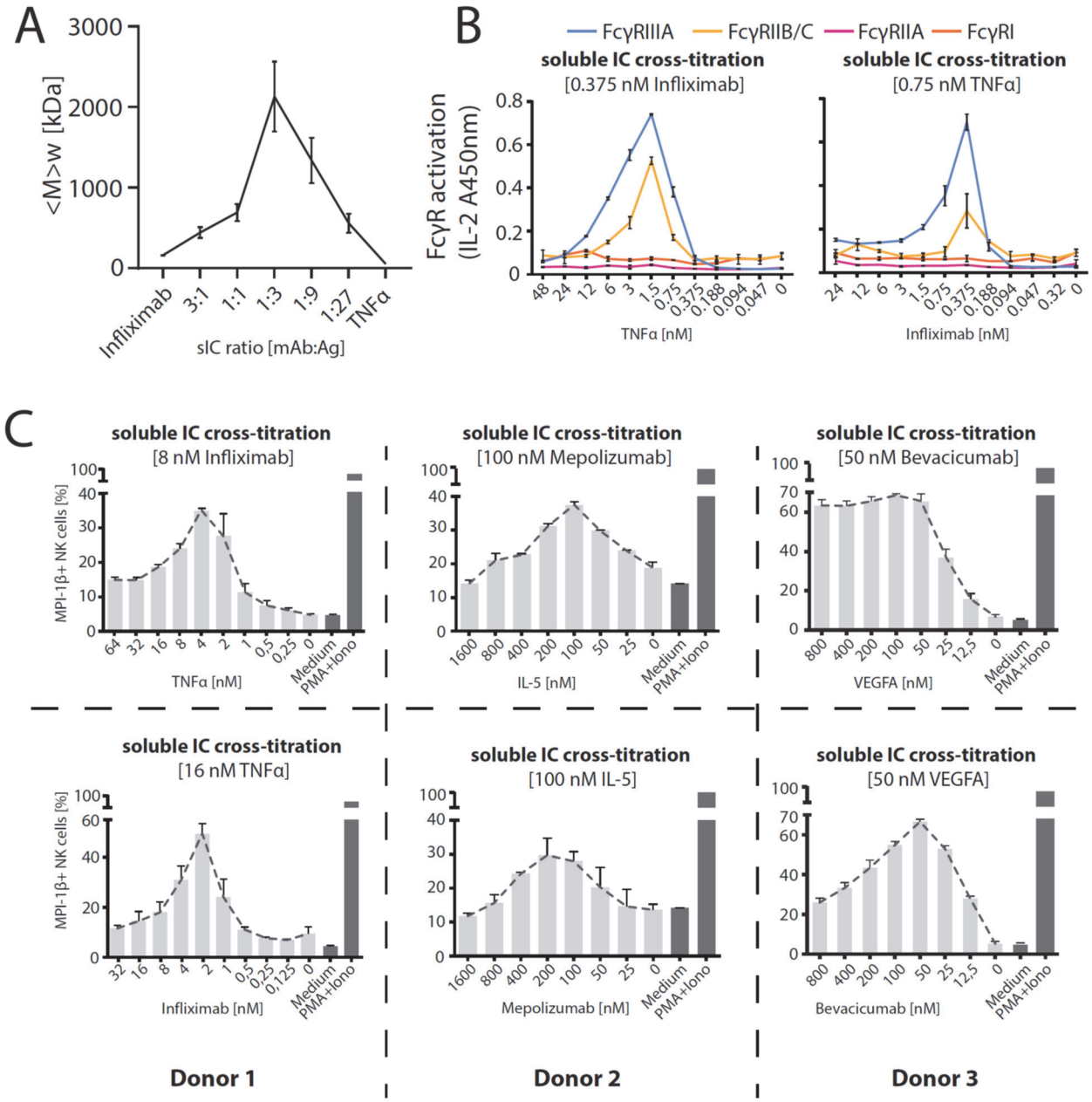

805

806

Fig. 5. FcγRIIB/C and FcγR-IIIA respond to sIC size reproducing a Heidelberger-Kendall like precipitation curve. A) infliximab (mAb) and rhTNFα (Ag) were mixed at different ratios (17 µg total protein, calculated from monomer molarity) and analysed via AF4. sIC size is maximal at a 1:3 ratio of mAb:Ag and reduced when either mAb or Ag are given in excess. $\langle M \rangle_w$ = mass-weighted mean of the molar mass distribution. Three independent experiments. Error bars = SD. Data taken from Table S1. One complete run analysis is shown in Fig. S2. B) FcγR BW5147 reporter cell activation is sensitive to sIC size. sICs of different size were generated by cross-titration according to the AF4 determination. Reporter cells were incubated with fixed amounts of either mAb (infliximab, left) or Ag (rhTNFα, right) and titrated amounts of antigen or antibody, respectively. X-Axis shows titration of either antigen or antibody, respectively (TNFα calculated as monomer). IL-2 production of reporter cells shows a peak for FcγRIIB/C and FcγRIIIA activation at an antibody:antigen ratio between 1:2 and 1:4. FcγRs I and IIA show no activation towards sICs in line with previous observations, see Fig.3. Two independent experiments. Error bars = SD. C) Purified primary NK cells from three different donors were incubated with cross-titrated sICs as in A. NK cells were measured for MIP-1β expression (% positivity). Incubation with PMA and Ionomycin served as a positive control. Incubation with medium alone served as a negative control. Measured in technical replicates. Error bars = SD.

825 **Figure 6**

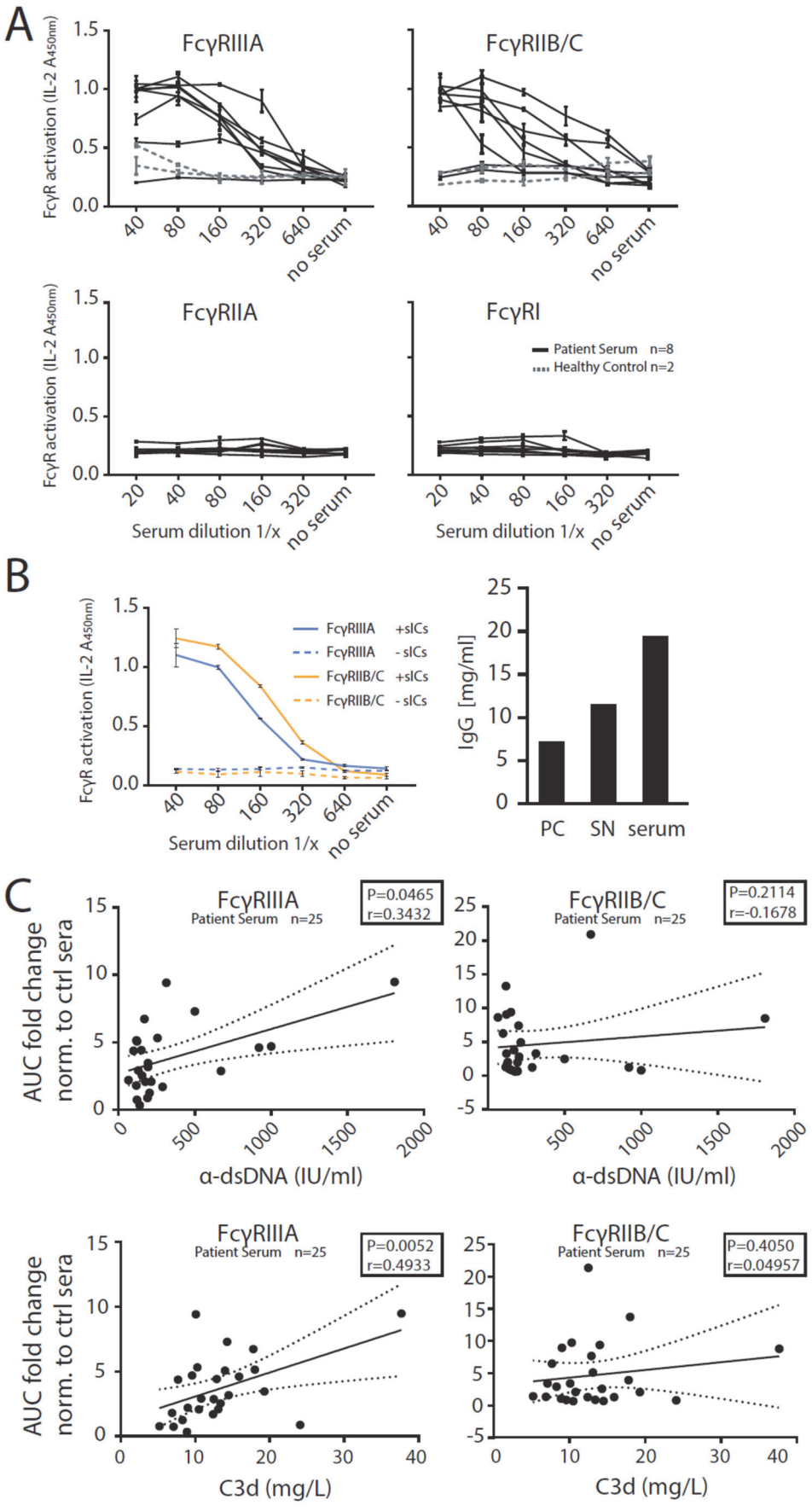

826

827 **Fig. 6. The reporter assay enables quantification of serum-derived sICs from SLE**
828 **patients.** Serum derived sIC from systemic lupus erythematosus (SLE) patients activate
829 human FcγR reporter cells. 25 patients and 4 healthy control individuals were separated into
830 three groups for measurement. A) Experiments shown for an exemplary group of 8 SLE
831 patients and two healthy individuals. Dose-dependent reactivity of FcγRs IIIA and IIB/C was
832 observed only for SLE patient sera and not for sera from healthy individuals. FcγRs I and IIA
833 show no reactivity towards clinical IC in line with previous observations. B) Activation of
834 FcγRs IIB/C and IIIA by patient serum is mediated by serum derived sICs. Patient serum
835 samples were depleted of sICs by PEG precipitation and the supernatant (SN) was compared
836 to untreated serum regarding FcγR activation (left). Performed in technical replicates. IgG
837 concentration in the precipitate (PC), supernatant (SN) or unfractionated serum respectively is
838 shown in the bar graph (right). IC precipitation did leave non-complexed IgG in the
839 supernatant. C) FcγRIIIA activation, but not FcγRIIB/C activation, significantly correlates
840 with known SLE disease markers. FcγR activation data from A was correlated to established
841 SLE disease markers (α-dsDNA levels indicated as IU/ml or C3d concentrations indicated as
842 mg/L). FcγR activation from a dose-response curve as in A was calculated as area under curve
843 (AUC) for each SLE patient (n=25) or healthy individual (n=4) and expressed as fold change
844 compared to the healthy control mean. SLE patients with α-dsDNA levels below 50 IU/ml
845 and C3d values below 6 mg/L were excluded. One-tailed Spearman's.
846
847

848 **Figure 7**

849

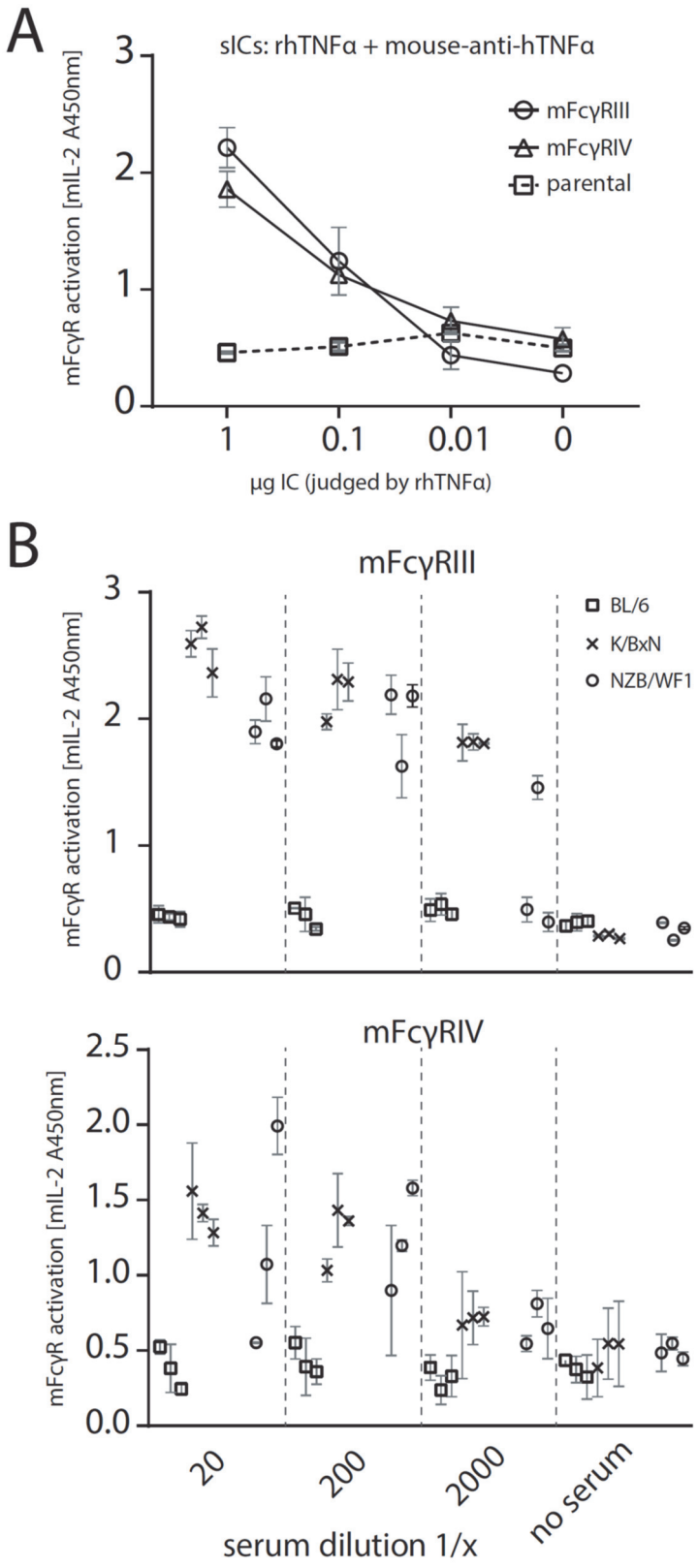

850

851

852 **Fig. 7. The reporter assay can be applied to mouse models of autoimmune disease.** A)
853 Reporter cells expressing mFcγRIII, mFcγRIV or parental BW5147 cells were incubated with
854 titrated amounts of synthetic sICs generated from rhTNFα and mouse-anti-hTNFα at a 1:1
855 ratio by mass. One experiment in technical replicates. Error bars = SD. B) Titrations of 3
856 mouse sera per group (C57BL/6, K/BxN or NZB/WF1) were incubated with mFcγR reporter
857 cells and FcγR activation was assessed as described above. Sera from BL/6 mice served as
858 negative control. Performed in technical replicates. Error bars = SD.
859
860

-Supplementary Material-

Figure S1

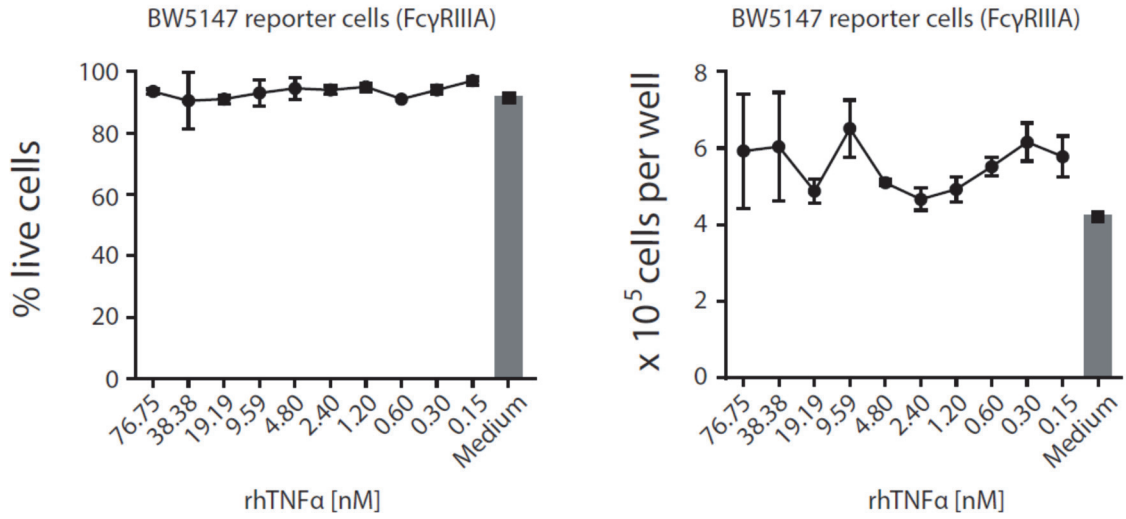

Fig. S1. rhTNFα is not toxic to mouse lymphocyte BW5147 cells even at high concentrations. Cell count and percentage of live cells were unaltered over a 16 h time frame of reporter cell culture in the presence of indicated rhTNFα concentrations and comparable to regular growth in complete medium. Experiments were conducted in 3 replicates. Error bars = SD.

873 **Figure S2**

874

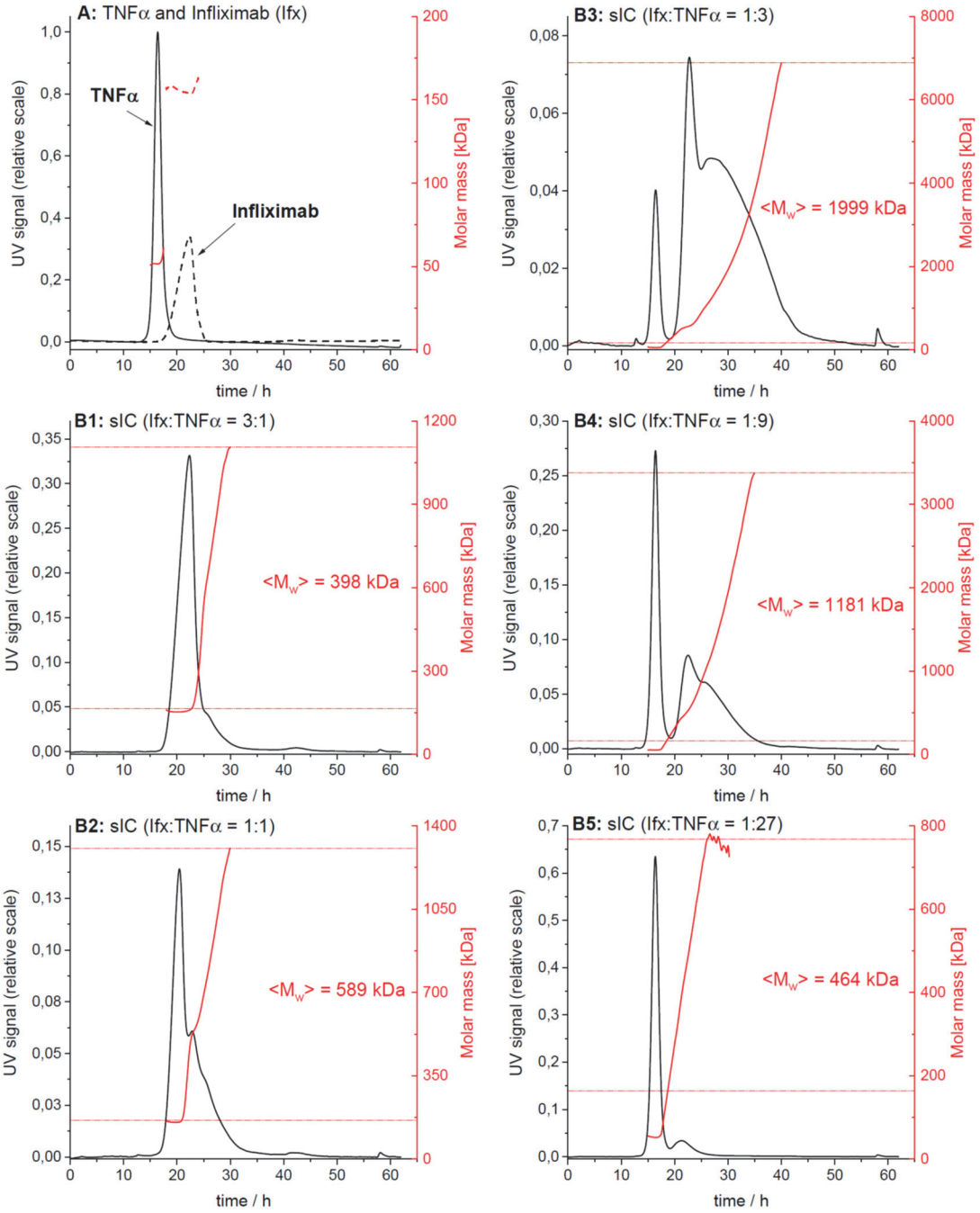

875

876

Fig. S2. AF4 elution profiles of Ifx/TNFα-immune complexes.

The elution profiles from one of three independent runs are shown. Protein concentration in the eluate is shown in black (UV signal at λ = 280 nm, normalized to the highest UV signal found in this experiment), molar masses determined by MALS for a given retention time in red. Horizontal red lines indicate the range of molar masses used to calculate the mass-weighted mean of molar masses $<M_w>$. A) Overlay of the elution profiles obtained for TNFα and Ifx, respectively; B1 to B5) Elution profiles for sICs formed after incubation of TNFα and Ifx at different molar ratios.

Table S1

Sample	Range of assigned molar masses [kDa]			Mass-weighted mean of assigned molar masses [kDa]			
	Run 1	Run 2	Run 3	Run 1	Run 2	Run 3	Mean ± SD
Infliximab, IFX	158 – 182	153 – 164	159 – 193	162	156	163	160 ± 4
TNF -alpha	52 – 55	51 – 61	52 – 62	52	52	52	52 ± 0
Immune complexes							
IFX/TNF 3:1	182 – $1.16 \cdot 10^3$	164 – $1.11 \cdot 10^3$	193 – $1.10 \cdot 10^3$	409	398	518	442 ± 66
IFX/TNF 1:1	182 – $2.06 \cdot 10^3$	164 – $1.31 \cdot 10^3$	193 – $1.42 \cdot 10^3$	801	589	681	690 ± 106
IFX/TNF 1:3	182 – $5.05 \cdot 10^3$	164 – $6.89 \cdot 10^3$	193 – $10.8 \cdot 10^3$	$1.77 \cdot 10^3$	$2.00 \cdot 10^3$	$2.61 \cdot 10^3$	$2.13 \cdot 10^3 \pm 435$
IFX/TNF 1:9	182 – $5.36 \cdot 10^3$	164 – $3.38 \cdot 10^3$	193 – $3.51 \cdot 10^3$	$1.66 \cdot 10^3$	$1.18 \cdot 10^3$	$1.17 \cdot 10^3$	$1.34 \cdot 10^3 \pm 279$
IFX/TNF 1:27	182 – $1.68 \cdot 10^3$	164 – 768	193 – $1.01 \cdot 10^3$	689	464	521	558 ± 117

Table S1. Analysis of the molar mass distribution of ICs from AF4 data.

For a given elution time, the AF4 profiles provide the concentration (UV) at which a given molar mass (MALS) of a protein is present in the sample. The molar mass distribution of Ifx, TNFα and their immune complexes (sICs) was obtained by plotting the cumulative frequency as a function of molar mass. For a selected range of molar masses, a mass-weighted mean value ($<M_w>$) was calculated. All detected molar masses were selected in the case of Ifx and TNFα whereas only molar masses larger than the maximal molar mass found for Ifx were assigned to sICs. The table shows the range of assigned molar masses and the calculated $<M_w>$ for each AF4 run (n = 3).